

TrackFormer: Multi-Object Tracking with Transformers

Tim Meinhardt^{1*} Alexander Kirillov² Laura Leal-Taixé¹ Christoph Feichtenhofer²

¹Technical University of Munich

²Facebook AI Research (FAIR)

Abstract

We present *TrackFormer*, an end-to-end multi-object tracking and segmentation model based on an encoder-decoder Transformer architecture. Our approach introduces track query embeddings which follow objects through a video sequence in an autoregressive fashion. New track queries are spawned by the DETR object detector and embed the position of their corresponding object over time. The Transformer decoder adjusts track query embeddings from frame to frame, thereby following the changing object positions. *TrackFormer* achieves a seamless data association between frames in a new tracking-by-attention paradigm by self- and encoder-decoder attention mechanisms which simultaneously reason about location, occlusion, and object identity. *TrackFormer* yields state-of-the-art performance on the tasks of multi-object tracking (MOT17) and segmentation (MOTS20). We hope our unified way of performing detection and tracking will foster future research in multi-object tracking and video understanding. Code will be made publicly available.

1. Introduction

Humans need to focus their *attention* to spatially track objects in time, for example, when playing a game of tennis, golf, or pong. This challenge is only increased when tracking not one, but *multiple* objects, in crowded real world scenarios. Following this analogy, we demonstrate the effectiveness of transformer attention for the task of multi-object tracking (MOT) in videos.

The goal in MOT is to follow the trajectories of a set of objects, *e.g.*, pedestrians, while keeping their identities discriminated as they are moving throughout a video. With progress in image-level object detectors [34, 7], most approaches follow the *tracking-by-detection* paradigm which consists of two-steps: (i) detecting objects in individual video frames, and (ii) associating sets of detections between frames, thereby creating individual object tracks over time.

*Work done during an internship at Facebook AI Research.

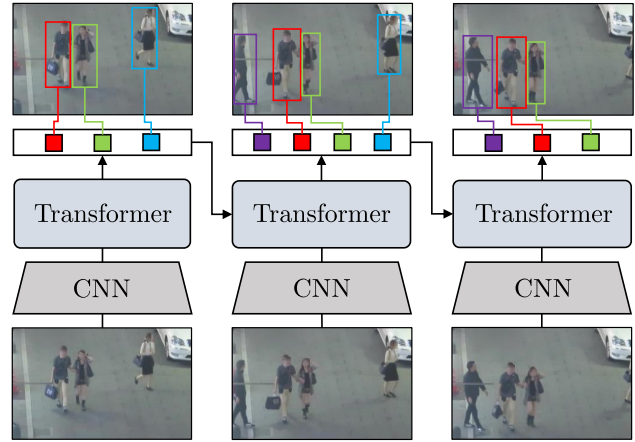


Figure 1. TrackFormer performs joint object detection and tracking by attention. Autoregressive track query embeddings connect past and future frames with Transformer based attention which reasons about identity, occlusion and detection of new objects.

Many MOT approaches differ in how they accomplish the second so-called *data association* step. Traditional tracking-by-detection methods associate detections via temporally sparse [21, 24] or dense [20, 17] graph optimization, or apply convolutional neural networks to predict matching scores between detections [8, 22].

Recent works [4, 6, 26] suggested a variation of the traditional paradigm coined as *tracking-by-regression* [12]. In this approach, the object detector not only provides frame-wise detections, but replaces the data association step with a continuous regression of each track to the changing position of its object. These approaches achieve track association implicitly but either rely on additional graph optimization [6, 26] or motion and appearance models [4] to achieve top performance. This is largely due to a lacking notion of object identity and local bounding box regression.

In this work, we present *TrackFormer*, a state-of-the-art approach to tackle MOT via *tracking-by-attention*. Our model simultaneously performs object detection and data association in a *unified way*. As illustrated in Fig. 1, *TrackFormer forms* trajectories over multiple frames with a convolutional neural network (CNN) [16] and Transformer [44] architecture based on the DETR [7] detector.

Our approach includes the novel concept of *track queries* which follow an object in space and time over the course of a video sequence in an autoregressive fashion. At each frame, the model transforms a set of track query embeddings representing the spatial position of their corresponding object. A Transformer performs *attention* operations over frame-level features and track queries to reason about object locations and identities as well as occlusions and emergence of new objects. The latter is accomplished in a unified way by the same Transformer spawning new track queries for objects entering the scene. The TrackFormer model is trained end-to-end by jointly optimizing detection and tracking in a set based prediction objective [42, 7]. It achieves track association implicitly with attention and requires no additional matching, optimization, or modeling of motion and appearance.

In empirical evaluation, we apply TrackFormer to the MOT17 [27] benchmark where it achieves state-of-the-art performance. Furthermore, we demonstrate the flexibility of our model to output segmentation masks and show state-of-the-art results on the Multi-Object Tracking and Segmentation (MOTS20) challenge [45].

In summary, we make the following **contributions**:

- A unified detection (or segmentation) and multi-object tracking approach with Transformers which achieves track association solely with attention in a new tracking-by-attention paradigm.
- The novel concept of autoregressive track queries which embed an object’s spatial position while following it over time.
- State-of-the-art results on two challenging multi-object tracking benchmarks (MOT17 and MOTS20).

2. Related work

In light of the recent trend to look beyond data association with detections, we categorize and review methods according to their respective tracking paradigm.

Tracking-by-detection approaches form trajectories by associating detections in time.

Graphs have been used for track association and long-term re-identification formulated as maximum flow (minimum cost) [3] problems with distance based [19, 32, 51] or learned costs [23]. Other methods use association graphs [41], learned models [21], and motion information [20], general-purpose solvers [50], multi-cuts [43], weighted graph labeling [17], edge lifting [18], or trainable graph neural networks [6]. However, graph-based approaches suffer from expensive optimization routines, limiting practical application for online tracking.

Appearance driven methods capitalize on increasingly powerful image recognition backbones to track with Siamese similarity [22], learned reID features [37], detection candidate selection [8] or affinity estimation [10]. As for re-identification, appearance models struggle in crowded scenarios with many object-object-occlusions.

Motion can be modelled for trajectory prediction [24, 1, 38] using a constant velocity assumption (CVA) [9, 2], the social force model [39, 31, 47, 24] which incorporates pedestrian movement and interactions, learned from data [23]. A learned motion model can also accomplish track association between frames [52]. In [53], objects are represented as center points which allow for an association by a distance-based greedy matching algorithm.

Tracking-by-regression approaches, spawn new trajectories by detection and, instead of associating individual detections between frames, accomplishes tracking by regressing the past locations to the new positions in the present frame. Previous efforts [13, 4] use regression heads on region pooled object detection features for box based association. To overcome the lack of object identity information of this approach, re-identification and motion models [4], as well as traditional [26] and learned [6] graph methods have been used on top of the tracking-by-regression paradigm.

Tracking-by-segmentation predict segmentation masks to benefit from pixel-level information to mitigate common appearance issues arising from crowdedness and ambiguous background areas. Prior attempts have used category-agnostic image segmentation [29], applied Mask R-CNN [15] with 3D convolutions [45] and mask pooling layers [33], or represent object masks as unordered point clouds [46].

Attention for image recognition. The self-attention mechanism used in Transformers [44] correlates information for each element of the input with respect to the others. Recently, Transformer based architectures are applied to various tasks such as image generation [30] and object detection [7]. For tracking, the general concept of attention has previously been applied to MOT tasks [54, 11]; however, these methods use attention only for the association of object detections. Our approach performs tracking *and* detection based on attention to *uniformly* reason out occlusion, track initialization and spatiotemporal correspondence.

3. TrackFormer

We present TrackFormer, a unified formulation for object detection (or segmentation) and multi-object tracking (MOT) with Transformers. This section first describes the

recently introduced concept of object detection with Transformers followed by the introduction of *track queries* and how these are trained for a frame to frame track generation in a new *tracking-by-attention* paradigm.

3.1. Detection with Transformers

In order to achieve object detection and tracking jointly, we build upon DETR [7], which uses an encoder-decoder transformer architecture to cast the object detection task as a set prediction problem. The detector yields object bounding boxes and class predictions for a single video frame in four consecutive steps:

- (i) Frame-level feature extraction with a common CNN backbone (*e.g.* ResNet [16]).
- (ii) Encoding of frame features with self-attention in a transformer encoder [44].
- (iii) Decoding of output embeddings with self- and encoder-decoder attention in a transformer decoder.
- (iv) Mapping of output embeddings to box and class predictions by multilayer perceptrons (MLP).

The Transformer decoder outputs a fixed set of N_{object} embeddings for potential object detections in the frame. It alternates between self- and encoder-decoder-, *i.e.*, frame-features-to-output-embeddings, attention. The latter attends each output globally to all frame features.

The permutation invariance of Transformers requires additive positional and object encodings for the frame features and output embeddings, respectively. Object encoding is achieved by initializing the output embeddings with N_{object} learned object encodings referred to as *object queries*.

Intuitively, each object query learns to predict objects with certain spatial properties (bounding box size and position). Over multiple consecutive decoding layers, these output embeddings accumulate bounding box and class information. The decoder self-attention relies on the object encoding to avoid duplicate detections and reason about spatial and categorical relations of objects.

Set prediction loss. During training, the predictions $\hat{y} = \{\hat{y}_i\}_{i=1}^{N_{\text{object}}}$ from step (iv) are assigned to one of the ground truth objects y or the background class. By design, the number of queries N_{object} exceeds the maximum number of ground truth objects per frame. Each y_i represents a bounding box b_i and object class c_i . Next, a bipartite matching is computed with costs based on bounding box similarity and object class. In order to search for the injective minimum cost mapping $\hat{\sigma}$ from ground truth to prediction indices the following assignment problem

$$\hat{\sigma} = \arg \min_{\sigma} \sum_i^{|y|} \mathcal{C}_{\text{match}}(y_i, \hat{y}_{\sigma(i)}), \quad (1)$$

with index $\sigma(i)$ and pair-wise costs $\mathcal{C}_{\text{match}}$ between ground truth y_i and prediction \hat{y}_i is solved with a combinatorial optimization algorithm as in [42]. Given the ground truth class labels c_i and predicted class probabilities $\hat{p}_i(c_i)$ for output embeddings i , the matching cost $\mathcal{C}_{\text{match}}$ is defined as

$$\mathcal{C}_{\text{match}} = -\hat{p}_{\sigma(i)}(c_i) + \mathcal{C}_{\text{box}}(b_i, \hat{b}_{\sigma(i)}). \quad (2)$$

In contrast to the common cross-entropy loss, the class prediction cost does not apply log probabilities. The \mathcal{C}_{box} term penalizes bounding box differences by a linear combination of a ℓ_1 distance and a generalized intersection over union (IoU) [35] cost \mathcal{C}_{iou} :

$$\mathcal{C}_{\text{box}} = \lambda_{\ell_1} \|b_i - \hat{b}_{\sigma(i)}\|_1 + \lambda_{\text{iou}} \mathcal{C}_{\text{iou}}(b_i, \hat{b}_{\sigma(i)}). \quad (3)$$

with weighting parameters $\lambda_{\ell_1}, \lambda_{\text{iou}} \in \mathfrak{R}$. The scale-invariant IoU term provides similar relative errors for different box sizes and mitigates inconsistency of ℓ_1 distance.

The final object detection (set prediction) loss is computed over all N_{object} output predictions:

$$\mathcal{L}_{\text{set}}(y, \hat{y}, \hat{\sigma}) = \sum_{i=1}^{N_{\text{object}}} \mathcal{L}_{\text{object}}(y, \hat{y}_i, \hat{\sigma}). \quad (4)$$

The subset of predictions \hat{y} which was not matched in (1) are not element of the mapping $\hat{\sigma}$ and will be assigned to the background class $c_i = 0$. We indicate the ground truth object matched with prediction i by $y_{\hat{\sigma}=i}$ and define the loss per object prediction

$$\mathcal{L}_{\text{object}} = \begin{cases} -\log \hat{p}_i(c_{\hat{\sigma}=i}) + \mathcal{L}_{\text{box}}(b_{\hat{\sigma}=i}, \hat{b}_i), & \text{if } i \in \hat{\sigma} \\ -\log \hat{p}_i(0), & \text{if } i \notin \hat{\sigma}. \end{cases}$$

The bounding box loss \mathcal{L}_{box} is computed in the same fashion as (3), but, we differentiate its terminology as the cost term \mathcal{C}_{box} is generally not required to be differentiable.

We next describe the generalization of this formulation for joint detection and tracking in video.

3.2. Track query

The multi-object tracking (MOT) task extends single image detection to multi frame track prediction. Given a video sequence with K individual object identities, MOT describes the task of generating ordered tracks $T_k = \{b_{t_1}^k, b_{t_2}^k, \dots\}$ with bounding boxes b_t and track identities k . The frames $\{t_1, t_2, \dots\}$ indicate the subset of frames an object appears in the sequence. This includes object-object and background-object occlusions.

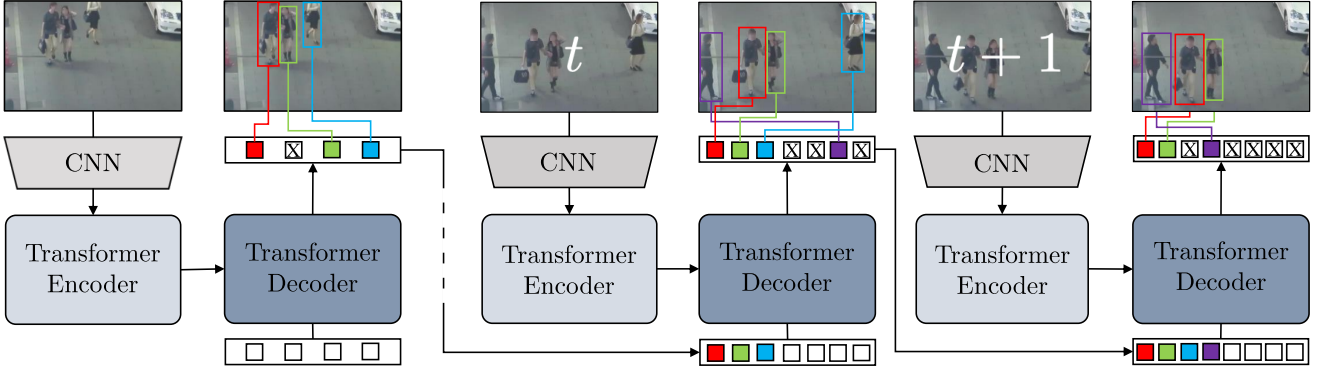


Figure 2. **TrackFormer** performs joint detection and multi-object tracking by autoregressively processing video. The architecture builds upon the DETR detector [7] and consists of a CNN for image feature extraction, a Transformer [44] encoder for image feature encoding and a Transformer decoder which applies self- and encoder-decoder attention to produce output embeddings with bounding box and class information. At frame $t = 0$, the decoder transforms N_{object} object queries (white) to output embeddings either initializing new **track queries** or predicting the background class (crossed). On subsequent frames, the decoder processes the joint set of $N_{\text{object}} + N_{\text{track}}$ queries to follow or remove (blue) existing tracks as well as initialize new tracks (purple).

In order to achieve frame to frame track generation, we introduce the concept of *track queries* to the object detector’s decoding step. Each track query follows a single object through a video sequence carrying over its identity information while adapting to its changing position in an autoregressive manner. For this purpose, the Transformer decoder performs attention on current frame features and previous frame track queries, to *continuously update* the representation of object identity and location in each track query embedding.

In Fig. 2, we provide a more concrete illustration of our concept. It shows how the initial detection in frame $t = 0$ spawns new track queries following their corresponding object to frame t and beyond. At frame $t = 0$, the detector yields N_{object} output embeddings for potential objects detections. Each successful object detection, *i.e.*, output embedding not predicting the background class, initializes a new track query embedding. For the decoding step at frame $t > 0$, each track query initializes an additional output embedding; therefore, the joint set of $N_{\text{object}} + N_{\text{track}}$ output embeddings is initialized by (learned) object and (temporally regressed) track queries, respectively. The Transformer decoder then transforms the entire set of output embeddings at once yielding bounding box and class predictions for frame t . The original detection objective (4) becomes a detection and tracking formulation

$$\mathcal{L}_{\text{set}}(y, \hat{y}, \hat{\sigma}) = \sum_{i=1}^{N_{\text{object}} + N_{\text{track}}} \mathcal{L}_{\text{object}}(y, \hat{y}_i, \hat{\sigma}). \quad (5)$$

New objects initializing additional tracks are detected by the N_{object} object query outputs. Note that, in contrast to the fixed set of learned object queries, track queries are *dynamic* and relay the previous frame output embeddings of their corresponding trajectory to the current frame.

Tracking and detection with queries. Our tracking procedure can be interpreted as a continuous *re-detection* of tracked objects, based on adaptively *regressing track queries*. Both, the learned and tracked, query types represent spatial properties of potential detections in frame t . Track queries allow for a frame to frame tracking by providing instance-specific information to the decoder. Self-attention over the joint set of track and object queries allows for the detection of new objects while simultaneously avoiding any re-detection of already tracked objects.

The temporal structure of videos allows for an *autoregressive* processing of previous output embeddings in the form of track queries. Following an object over the course of a sequence, its corresponding track query embedding is dynamically updated by the decoder. TrackFormer thereby achieves implicit multi-frame attention which benefits the frame to frame object tracking performance.

By default, the track query concept incurs no parameter overhead for the architecture, but track queries might require additional adaptation before being merged with the object queries for joint detection and tracking. We add an explicit *track query attention* block to the decoder that is transforming the previous frame track queries for processing in the current frame. A detailed architecture overview is in Fig. A.1 of the appendix, where we illustrate the integration of track queries and the additional self-attention block in the decoder of the detection and tracking architecture.

3.3. TrackFormer training

For track queries to follow objects to the next frame and work in interaction with the object queries, TrackFormer requires dedicated frame-to-frame tracking training. For this, we train on two adjacent frames, as indicated in Fig. 2, and optimize for object detection and tracking at frame t . The joint objective corresponds to the set prediction loss in

Eq. (5) and measures the set prediction of all output embeddings $N_{\text{object}} + N_{\text{track}}$ with respect to the ground truth objects in terms of class prediction and bounding box similarity.

The set prediction loss is computed in two steps:

- (i) Object detection on frame $t - 1$ as in (4) with N_{object} object queries (see $t = 0$ in Fig. 2).
- (ii) Tracking of objects from (i) and detection of new objects on frame t as in (5) with $N_{\text{object}} + N_{\text{track}}$ queries.

The number of track queries N_{track} depends on the number of successfully detected objects in frame $t - 1$.

Bipartite track query matching. As outlined in Sec. 3.1, the object detection (set prediction) loss for frame t is computed by matching the corresponding output predictions with ground truth objects. We denote the subset of ground truth track identities at frame t with $K_t \subset K$. Each detection from step (i) is assigned to its respective ground truth track identity k from the set $K_{t-1} \subset K$. The corresponding output embeddings, *i.e.* track queries, inherently carry over the identity information to the matching procedure in the next frame. The two ground truth track identity sets describe a hard assignment of the N_{track} track query outputs to the ground truth object in frame t :

$K_t \cap K_{t-1}$: Match by track identity k .

$K_{t-1} \setminus K_t$: Match with background class.

$K_t \setminus K_{t-1}$: No matching via track identity.

The second set of ground truth track identities $K_{t-1} \setminus K_t$ includes tracks which either have been occluded or left the scene at frame t . The last set $K_t \setminus K_{t-1}$ of previously not yet tracked objects remains to be matched with the N_{object} object queries. For this, we apply the bipartite cost-based matching described in Sec. 3.1.

Track augmentations. The two step training process for training track queries represents only a limited range of possible tracking scenarios. Therefore, we propose the following augmentations to enrich the set of potential track queries during training. These augmentations will be verified in our experiments. We use three types of augmentations which lead to perturbation of object location and motion, missing detections, and simulated occlusion.

1. The frame $t - 1$ for step (i) is sampled from a range of frames around frame t , thereby generating challenging frame pairs where the objects have moved substantially from their previous position. Such a sampling allows for the simulation of camera motion and low frame rates from usually benevolent sequences.

2. We sample false negatives with a probability of p_{FN} by removing track queries before proceeding with step (ii). The corresponding ground truth objects in frame t will be matched with object queries and trigger a new object detection. Keeping the ratio of false positives sufficiently high allows for a balanced training of both query types. Such a balance is crucial for our joint detection and tracking approach.
3. To improve the removal of tracks by assigning the background class in object occlusion scenarios, we complement the set of track queries with additional false positives. These queries are sampled from the output embeddings of frame $t - 1$ that were classified as background. Each of the original track queries has a chance of p_{FP} to spawn an additional false positive query. We chose these with a large likelihood of occluding with the respective spawning track query.

Another common augmentation for improved robustness, is to applying spatial jittering to input bounding boxes or center points [53]. The nature of track queries, which encode spatial object information implicitly, does not allow for such an explicit perturbation in the spatial domain. We believe our randomization of the temporal stride (augmentation type 1) provides a more natural augmentation from video to improve generalization.

3.4. MOT with TrackFormer

At inference time, TrackFormer starts MOT on a single video sequence as in Fig. 2 by predicting all objects $\{\mathbf{b}_0^0, \mathbf{b}_0^1, \dots\}$ of the first frame $t = 0$. Not all objects might appear on the first frame; therefore, the track identities $K_0 = \{0, 1, \dots\}$ only represent a subset of all K objects in a sequence. At frame $t + 1$, TrackFormer decodes $N_{\text{object}} + N_{\text{track}}$ output embeddings. The latter changes between frames as new objects are detected or tracks are removed. Object detections from one of the object queries initialize new tracks if their classification score is above $\sigma_{\text{detection}}$. Existing tracks followed by a track query can be removed either if their classification score drops below σ_{track} or by a Trajectory non-maximum suppression (NMS) with a very high IoU threshold of $\sigma_{\text{track-NMS}} = 0.9$ applied to all current tracks. Application of $\sigma_{\text{track-NMS}}$ removes duplicate boxes and can improve detection accuracy as track query embeddings of strongly overlapping cases are not resolvable by the decoder self-attention. We return to this in Sec. 4.4 of our experiments.

4. Experiments

In this section, we present tracking results for TrackFormer on two MOTChallenge benchmarks, namely, MOT17 [28] and MOTS20 [45]. Furthermore, we verify individual contributions in an ablation study.

4.1. MOT benchmarks and metrics

Datasets. MOT17 [28] has a train and test set, each with 7 sequences and pedestrians annotated with full-body bounding boxes. To evaluate the tracking (data association) robustness independently, three sets of public detections are provided, DPM [14], Faster R-CNN [34] and SDP [48].

MOTS20 [45] provides mask annotations for 4 train and test sequences of MOT17. The corresponding bounding boxes are not full-body, but based on the visible segmentation masks, and only large objects are annotated.

Metrics. Different aspects of MOT are evaluated by a number of individual metrics [5]. The community focuses on two compound metrics, namely, Multiple Object Tracking Accuracy (MOTA) and Identity F1 Score (IDF1) [36]. While the former focuses on object coverage, the identity preservation of a method is measured by the latter. For MOTS, we report MOTSA which evaluates predictions with a ground truth matching based on mask IoU.

4.2. Implementation details

TrackFormer follows the CNN feature extraction and Transformer encoder-decoder architecture presented in [7]. The former is achieved with a ResNet101 [16] backbone and both the encoder and decoder apply 6 individual layers of feature width 256. Each attention layer applies multi-headed self-attention [44] with 8 attention heads. We do not use the “DC5” (dilated conv₅) version of the backbone as this will incur a large memory requirement related to the larger resolution of the last residual stage. However, we expect “DC5” or any other heavier backbone, or higher-resolution, to improve results even further and leave this for future work.

Our training hyperparameters mostly follow the original DETR [7]. The weighting parameters of the individual box cost \mathcal{C}_{box} and loss \mathcal{L}_{box} are set to $\lambda_{\ell_1} = 5$ and $\lambda_{\text{iou}} = 2$.

Queries and the background class. By design, TrackFormer can only detect a maximum of N_{object} objects. To detect the maximum number of objects (52) per frame in MOT17 [27], we train TrackFormer with $N_{\text{object}} = 100$ learned object queries. The number of possible track queries is adaptive and only practically limited by the ability of the decoder to discriminate them. The total number of queries usually largely exceeds the number of ground truth objects per frame. To mitigate the resulting class imbalance, we downweigh the class prediction loss for background class queries by a factor of 0.1. We do not apply downweighting for false positive track augmentations to facilitate the training of track removal.

Training procedure. The object detector without track queries is pre-trained on COCO [25]. As in [7], the backbone and encoder-decoder are trained for 500 epochs with individual learning rates of 0.0001 and 0.00001, respectively. Both learning rates are dropped after 400 epochs by a factor of 10. The core tracking capabilities are trained by simulating adjacent MOT frames from single images. To this end, we fine-tune the pre-trained model for another 200 epochs on the person detection CrowdHuman [40] dataset (described next), similar to [53]. Finally, we drop the learning rates even further and train TrackFormer for another 200 epochs on MOT17 [27]. Excluding the COCO pretraining, we train TrackFormer for around 3 days on 8 16GB V100 GPUs.

Single image track training. The encoder-decoder multi-level attention mechanism requires substantial amounts of training data. Hence, we follow a similar approach as in [53] and simulate MOT data from the CrowdHuman [40] person detection dataset. For our training we filter out all images with more than 50 objects. The adjacent training frames $t - 1$ and t in Fig. 2 are generated by applying random spatial augmentations to a single image. To simulate high frame rate image pairs as in MOT17 [27], we randomly resize and crop of only up to 0.05% with respect to the original image size.

Mask training. TrackFormer predicts instance-level object masks in a segmentation head as in [7] by generating spatial attention maps from the encoded image features and decoder output embeddings. These are followed by up-scaling and convolution operations to yield mask predictions for all decoder output embeddings. Since MOT17 and MOTS20 [45] have several sequences in common, we adapt the same training pipeline. After training on MOT17, we freeze the model except from the segmentation head which is trained on all COCO images containing people. Finally, we fine-tune the entire model on the MOTS20 dataset. This adapts the model to the MOTS20 ground truth which differs from MOT17 by removing small objects and ones not including full body but segmentation based bounding boxes.

Public detection. The MOT17 [27] benchmark is evaluated in a public detection setting which allows for a comparison of tracking methods independent of the underlying object detection performance. MOT17 provides three sets of public detections with varying quality. In contrast to tracking-by-detection methods, TrackFormer is not able to directly produce tracking outputs from detection inputs. In the next section, we report the results in Tab. 1 by filtering the initialization of tracks with the same center point distance filter as in [53]. For more implementation details, a

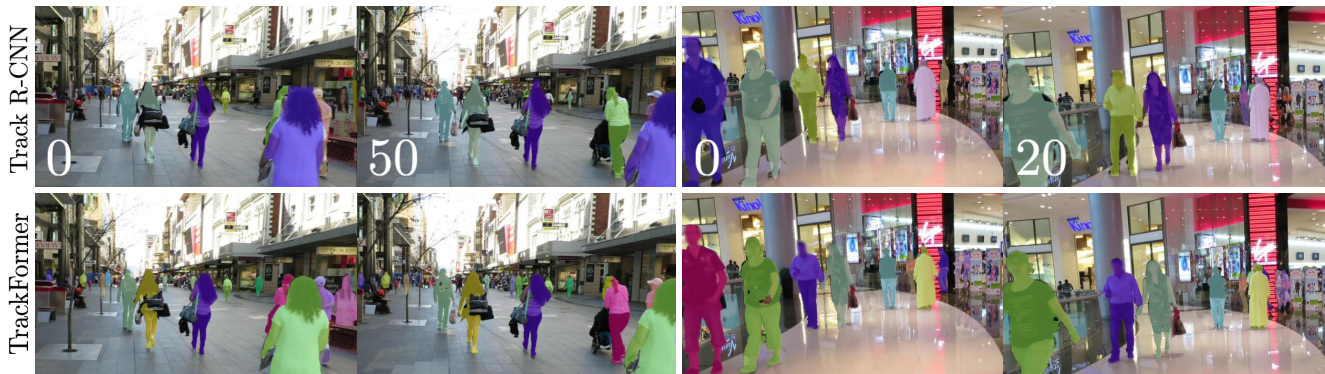


Figure 3. We compare TrackFormer segmentation results with the popular Track R-CNN [45] on selected MOTS20 [45] test sequences. The superiority of TrackFormer in terms of MOTSA in Tab. 2 can be clearly observed by the difference in pixel mask accuracy.

Method	MOTA \uparrow	IDF1 \uparrow	MT \uparrow	ML \downarrow	FP \downarrow	FN \downarrow	ID Sw. \downarrow
Offline							
MHT_DAM [21]	50.7	47.2	491	869	22875	252889	2314
jCC [20]	51.2	54.5	493	872	25937	247822	1802
FWT [17]	51.3	47.6	505	830	24101	247921	2648
eHAF [41]	51.8	54.7	551	893	33212	236772	1834
TT [52]	54.9	63.1	575	897	20236	233295	1088
MPNTrack [6]	58.8	61.7	679	788	17413	213594	1185
Lif_T [18]	60.5	65.6	637	791	14966	206619	1189
Online							
MOTDT [8]	50.9	52.7	413	841	24069	250768	2474
FAMNet [10]	52.0	48.7	450	787	14138	253616	3072
Tractor++ [4]	56.3	55.1	498	831	8866	235449	1987
GSM_Tractor [26]	56.4	57.8	523	813	14379	230174	1485
CenterTrack [53]	61.5	59.6	621	752	14076	200672	2583
TrackFormer	61.8	59.8	834	496	35226	177270	2982

Table 1. Comparison of modern multi-object tracking methods evaluated on the MOT17 [27] test set. We report mean results over the three sets of public detections provided by [27] and separate between online and offline approaches. TrackFormer achieves state-of-the-art results in terms of MOTA among all tracking methods. The arrows indicate low or high optimal metric values.

discussion on public detections and the fairness of such a filtering, we refer to appendix B.1.

4.3. Main results

MOT17. Following the training procedure described in Sec. 4.2, we evaluate TrackFormer on the MOT17 [27] test set and report results in Tab. 1. We achieve state-of-the-art results in terms of MOTA in a public setting for online and offline tracking methods. Our runtime (Hz) and identity preservation performance (IDF1, ID Sw.) is comparable to other online approaches. The latter is only surpassed by offline methods which reason about identity by processing sequences at once. TrackFormer achieves top performance by applying global attention to all input pixels without relying on additional motion [4, 10] or appearance models [4, 8, 10]. Furthermore, the frame to frame association

Method	TbD	sMOTSA \uparrow	IDF1 \uparrow	FP \downarrow	FN \downarrow	ID Sw. \downarrow
Train set (4-fold cross-validation)						
MHT_DAM [21]	×	48.0	–	–	–	–
FWT [17]	×	49.3	–	–	–	–
MOTDT [8]	×	47.8	–	–	–	–
jCC [20]	×	48.3	–	–	–	–
TrackRCNN [45]		52.7	–	–	–	–
MOTNet [33]		56.8	–	–	–	–
PointTrack [46]		58.1	–	–	–	–
TrackFormer		58.7	–	–	–	–
Test set						
Track R-CNN [45]		40.6	42.4	1261	12641	567
TrackFormer		54.9	63.6	2,233	7,195	278

Table 2. Comparison of modern multi-object tracking and segmentation methods evaluated on the MOTS20 [45] train and test sets. Methods indicated with *TbD* originally perform tracking-by-detection without segmentation. Hence, they are evaluated on SDP [49] public detections and predict masks with an additional Mask R-CNN [15] fine-tuned on MOTS20. TrackFormer achieves state-of-the-art results in terms of MOTSA and IDF1 on both sets.

with track queries avoids any post-processing with heuristic matching procedures [53] or graph optimization [26].

MOTS20. In addition to object detection and tracking, TrackFormer is able to predict instance-level segmentation masks. We follow the same training pipeline as for MOT17 but with additional segmentation head training on MOTS20 [45]. As reported in Tab. 2, we achieve state-of-the-art MOTS results in terms of object coverage (MOTSA) and identity preservation (IDF1). All methods are evaluated in a private setting. A MOTS20 test set submission is only possible since recently, hence we also provide the 4-fold cross-validation evaluation established in [45] and report the mean best epoch results over all splits. TrackFormer surpasses all previous methods without a dedicated tracking formulation for segmentation masks as in [46]. In Fig. 3, we present a qualitative comparison of TrackFormer and Track R-CNN [45] on two test sequences of MOTS20 [45].

Method	MOTA \uparrow	Δ	IDF1 \uparrow	Δ
TrackFormer	54.6		53.8	
w/o				
Track query attention	53.3	-1.3	51.4	-2.4
Track augmentations	52.4	-2.2	49.8	-4.0
Track query	48.5	-6.1	19.8	-34.0

Table 3. Ablation study on individual TrackFormer components. We report mean best epoch results in a private setting on a 3-fold split on the MOT17 [27] training set. For the last row without (w/o) all components, we train DETR [7] only for object detection and associate tracks based on output embedding distance.

Method	MOT17	CrowdHuman	MOTA \uparrow	IDF1 \uparrow
DETR [7]	\times	\times	48.5	19.8
	\times		41.5	19.1

Table 4. Ablation study on the performance gain from training on the CrowdHuman dataset. We train DETR [7] only for object detection and associate tracks based on output embedding distance. The first row corresponds to the last row in Tab. 3.

4.4. Ablation study

The ablations on MOT17 are evaluated with a 3-fold cross-validation split on the train set as described in [6].

TrackFormer components. We ablate the impact in tracking performance for different components of TrackFormer in Tab. 3. Our full system provides a MOTA of 54.6 and IDF1 of 53.8. The baseline without (w/o) our *track query attention* reduces this by -1.3 and -2.4 points, respectively. We found this explicit self-attention over track queries in each decoding layer to improve results as the general reasoning about object detection differs from the challenge of keeping the track identity to track query mapping unchanged. If we further ablate our *track augmentations* during training, we see another drop of -2.2 and -4.0 points. Finally, the baseline without (w/o) all tracking components does not use *track queries* and performs association based on output embedding distance of the object detector. In the last row of Tab. 3, we see a dramatic decay of -6.1 and -34.0 in MOTA and IDF1 for this variant, respectively.

Single image pretraining. Pretraining on additional datasets which do not provide frame to frame tracking ground truth data, such as the CrowdHuman [40] dataset, is common for MOT methods [53, 4, 8]. All versions in Tab. 3 are pretrained on the CrowdHuman [40] dataset. In Tab. 4, we observe that the predominant effect of such a pretraining improves object coverage (MOTA) in the baseline of Tab. 3 which does not use our tracking components. Despite the addition of CrowdHuman, the baseline still fails to properly associate tracks over frames (IDF1 is relatively unchanged).

Method	NMS detection	NMS tracking	MOTA \uparrow	IDF1 \uparrow
	\times	\times	54.6	53.9
TrackFormer		\times	54.6	53.8
			51.7	53.0

Table 5. Ablation study on the application of non-maximum suppression (NMS) on the set of tracks and for the detection of new objects. The second row corresponds to the first row in Tab. 3.

Method	Mask training	MOTA \uparrow	IDF1 \uparrow
TrackFormer	\times	61.9	56.0
		61.9	54.8

Table 6. We demonstrate the effect of jointly training for tracking and segmentation on a 4-fold split on the MOTS20 [45] train set. We evaluate with regular MOT metrics, *i.e.*, matching to ground truth with bounding boxes instead of masks.

Non-maximum suppression. In Tab. 5, we evaluate the application of non-maximum suppression (NMS) to new object detections, or to the set of tracks. For new object detections, TrackFormer yields consistent results with or without NMS. For tracks, the intersection of trajectories can lead to strong occlusion cases and pose ambiguous track overlaps. If these are not removed by NMS from the set of tracks, objects might accumulate multiple track queries which hurts the MOTA performance (but has no impact on IDF1). The MOTA decay is caused by the inability of the decoder self-attention to spatially discriminate almost identical track query embeddings converging to the same target.

Segmentation improves tracking. This final ablation demonstrates how segmentation mask prediction can improve tracking performance. The effectiveness of a unified segmentation and tracking training procedure is shown in Tab. 6. In contrast to [7], we trained the entire model including the mask head which improves the tracking performance (IDF1), even when evaluated on bounding boxes.

5. Conclusion

We have presented a new unified end-to-end approach for detection and multi-object tracking with Transformers. Our TrackFormer architecture introduces track query embeddings which follow objects over a sequence in an autoregressive manner. A Transformer encoder-decoder architecture transforms each track query to the changing position of its corresponding object. TrackFormer associates tracks over time solely by attention operations and does not rely on any additional matching, graph optimization, motion or appearance modeling. Our approach achieves state-of-the-art results for multi-object tracking as well as segmentation. We hope that this new tracking-by-attention paradigm will foster future work in detection and tracking in video.

Acknowledgements: We are grateful for discussions with Jitendra Malik, Karttikeya Mangalam, and David Novotny.

Appendix

This section provides additional material for the main paper: §A contains additional implementation details for TrackFormer (§A.1), a visualization of the Transformer encoder-decoder architecture (§A.3), and parameters for multi-object tracking (§A.4). §B contains further results related to public detection filtering (§B.1), and detailed per-sequence results tables for MOT17 and MOTS20 (§B.2).

A. Implementation details

A.1. Backbone and training

We provide additional hyperparameters for TrackFormer. This supports our implementation details reported in Sec. 4.2 of the main paper. We use ResNet101 [16] as backbone and pre-train our model for COCO [25] object detection, following [7]. We do not use the “DC5” (dilated conv₅) version of the backbone as this will incur a large memory requirement related to the larger resolution of the last residual stage. We expect that using “DC5” or any other heavier, or higher-resolution, backbone to provide better accuracy and leave this for future work.

Our training hyperparameters mostly follow the original DETR [7]. The weighting parameters of the individual box cost \mathcal{C}_{box} and loss \mathcal{L}_{box} are set to $\lambda_{\ell_1} = 5$ and $\lambda_{\text{iou}} = 2$.

A.2. Dataset splits

All experiments evaluated on dataset splits (ablation studies and MOTS20 training set in Tab. 2) follow the same training pipeline presented in Sec. 4.2 applied to each split. We average all validation metrics over the splits and report the results from a single epoch (which yields the best mean MOTA / MOTSA) over all splits; *i.e.* we do not take the best epoch for each individual split. For our ablation on the MOT17 [27] training set, we follow [6] and separate the 7 sequences into 3 splits as shown in Tab. A.1 stratified by their number of frames, tracks and, the inclusion of camera movement. Before training each of the 4 MOTS20 [45] splits, we pre-train the model on all MOT17 sequences excluding the corresponding split of the validation sequence.

A.3. Transformer encoder-decoder architecture

To foster the understanding of how TrackFormer integrates track queries within the decoder self-attention block, we provide a visualization of the encoder-decoder architecture.

In Fig. A.1, we illustrate the detailed integration of track queries and the additional self-attention block into the DETR encoder-decoder architecture. In comparison to the

Name	CM	Length [s]	Length [f]	Tracks	Boxes
Split 1					
MOT17-02	No	20	600	62	18581
MOT17-10	Yes	22	654	57	12839
MOT17-13	Yes	30	750	110	11642
All	–	72	2004	229	43062
Split 2					
MOT17-04	No	35	1050	83	47557
MOT17-11	Yes	30	900	75	9436
All	–	65	1950	158	56993
Split 3					
MOT17-05	Yes	60	837	133	6917
MOT17-09	No	18	525	26	5325
All	–	78	1362	159	12242
Total					
	–	205	5316	546	112297

Table A.1. For our ablation studies, we follow the 3-fold cross-validation split on the MOT17 [27] training set presented in [6]. We indicate sequences including camera movement with *CM* and report their length in the number of seconds (s) and frames (f).

original illustration in [7], we indicate *track identities* instead of spatial encoding with *color-coded* queries. The frame features (indicated in grey) are the final output of the CNN feature extractor and have the same number of channels as both query types. The entire Transformer architecture applies N and M independently supervised encoder and decoder layers, with spatial positional and object encoding as in [7]. Track queries are fed *autoregressively* from the *previous frame* output embeddings of the last decoding layer (before the final feed-forward class and bounding box networks (FFN)). In the current frame, track queries are processed by a separate self-attention block and then concatenated (\oplus) with the object queries (an ablation of this extra *track query attention* block this is given in Tab. 3 of the main paper). The object encoding is achieved by re-adding the object queries to the corresponding embeddings in the decoder key (K) and query (Q) in the decoder.

A.4. Multi-object tracking parameters

In Sec. 3.4, we explain the process of track initialization and removal over a sequence. The corresponding classification score and intersection over union thresholds were optimized by a hyperparameter grid search on the MOT17 training set cross-validation split. The grid search yielded track initialization and removal threshold of $\sigma_{\text{detection}} = 0.9$ and $\sigma_{\text{track}} = 0.6$, respectively. The lower σ_{track} score prevents tracks from being removed too early and improves identity preservation performance significantly. As discussed in the non-maximum suppression (NMS) ablation (Sec. 4.4 of the

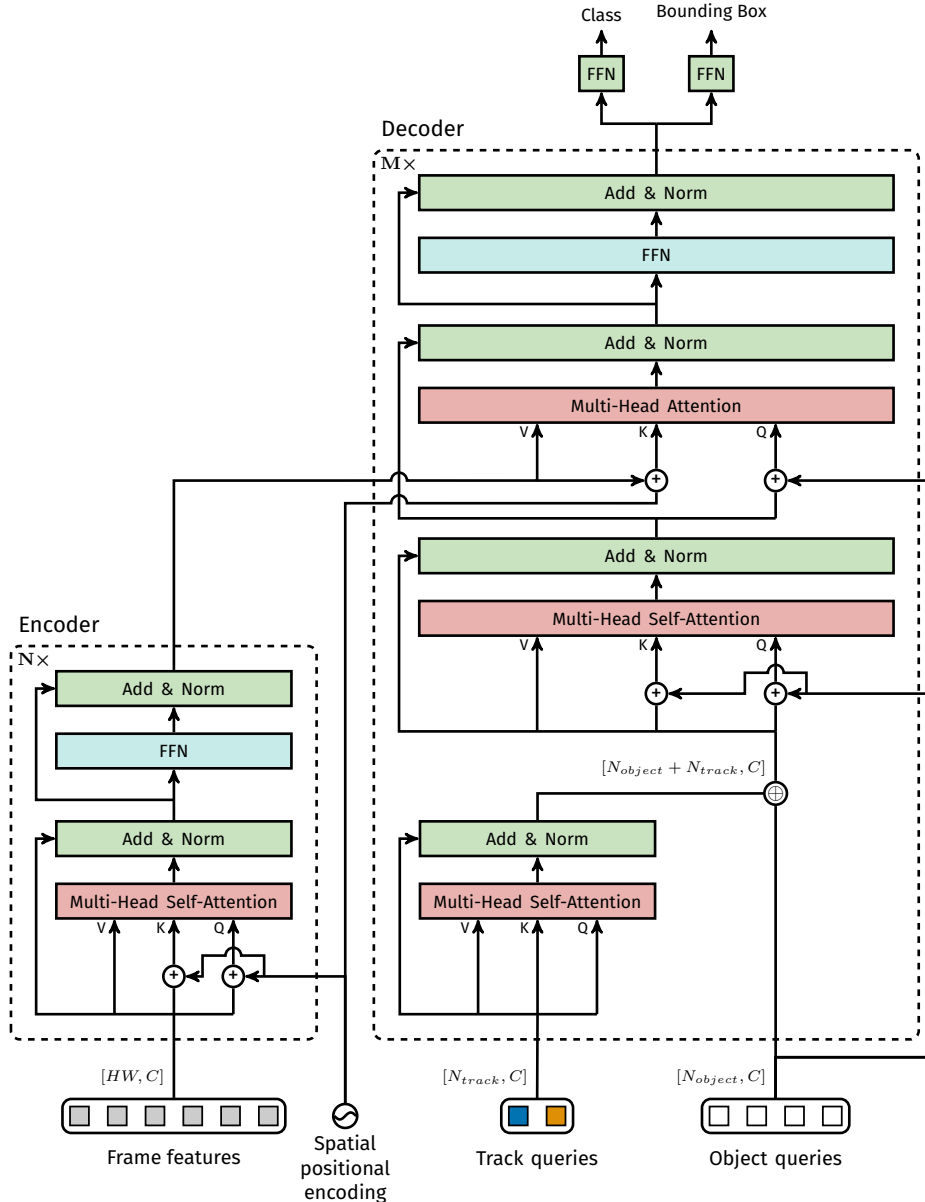


Figure A.1. The TrackFormer encoder-decoder architecture. We indicate the tensor dimensions in squared brackets.

main paper), TrackFormer benefits from an NMS operation for the removal of strong occlusion cases. (This NMS only removes highly overlapping bounding boxes with an intersection over union larger than $\sigma_{\text{track-NMS}} = 0.9$).

B. Experiments

B.1. Public detections and track filtering

TrackFormer implements a new tracking-by-attention paradigm which requires track initialization filtering to be evaluated with public detections. Here, we provide a discussion on the comparability of TrackFormer with earlier

methods and different filtering schemes.

Common tracking-by-detection methods directly process public detections and report their mean tracking performance on all three sets. This is only possible for methods that perform the data association step on a bounding box level. TrackFormer and point-based methods such as [53] require a procedure for filtering track initializations by public detections in a comparable manner. Unfortunately, MOT17 does not provide a standardized procedure for such a filtering. The authors of CenterTrack [53] filter based on bounding box center distances (CD). Each public detection initializes a single track only if its center falls in

Method	IN	IoU	CD	MOTA \uparrow	IDF1 \uparrow
Offline					
MHT_DAM [21]	\times			50.7	47.2
jCC [20]	\times			51.2	54.5
FWT [17]	\times			51.3	47.6
eHAF [41]	\times			51.8	54.7
TT [52]	\times			54.9	63.1
MPNTrack [6]	\times			58.8	61.7
Lif_T [18]	\times			60.5	65.6
Online					
MOTDT [8]	\times			50.9	52.7
FAMNet [10]	\times			52.0	48.7
Tracktor++ [4]	\times			56.3	55.1
GSM_Tracktor [26]	\times			56.4	57.8
TrackFormer		\times		59.7	59.0
CenterTrack [53]			\times	61.5	59.6
TrackFormer			\times	61.8	59.8

Table A.2. Comparison of modern multi-object tracking methods evaluated on the MOT17 [27] test set for different **public detection processing**. Public detections are either directly processed as input (IN) or applied for filtering of track initializations by center distance (CD) or intersection over union (IoU). We report mean results over the three sets of public detections provided by [27] and separate between online and offline approaches. The arrows indicate low or high optimal metric values.

Sequence	sMOTSA \uparrow	IDF1 \uparrow	MOTSA \uparrow	FP \downarrow	FN \downarrow	ID Sw. \downarrow
MOTS20-01	59.8	68.0	79.6	255	364	16
MOTS20-06	63.9	65.1	78.7	595	1335	158
MOTS20-07	43.2	53.6	58.5	834	4433	75
MOTS20-12	62.0	76.8	74.6	549	1063	29
ALL	54.9	63.6	69.9	2233	7195	278

Table A.3. We present TrackFormer tracking and segmentation results on each individual sequence of the MOTS20 [45] test set. MOTS20 is evaluated in a private detections setting. The arrows indicate low or high optimal metric values.

the bounding box area of the corresponding track. We followed this CD-based filtering to compare with CenterTrack.

In Tab. A.2, we revisit our MOT17 test set results with the same public detections center distance (CD) filtering, and also inspect the corresponding per-sequence results in Tab. A.4. We observe that this filtering does not reflect the quality differences in each set of public detections, *i.e.*, DPM [14] and SDP [48] results are expected to be the worst and best, respectively, but their difference is small.

Therefore, we deem a center distance filtering not to be in line with the common public detection setting and propose a filtering based on IoU. For TrackFormer with IoU filtering in Tab. A.2, public detections only initialize a track

if they have an IoU larger than 0.5. As expected this version performs worse compared to the CD filtering but we believe it provides a fairer comparison to previous MOT methods which directly process public detections as inputs (IN). The per-sequence results with IoU filtering in Tab. A.5, showing larger differences across detectors, support this statement.

B.2. MOT17 and MOTS20 sequence results

In Tab. A.4 and Tab. A.5, we provide per-sequence MOT17 [27] test set results for public detection filtering via center distance (CD) or intersection over union (IoU). Furthermore, we present per-sequence TrackFormer results on the MOTS20 [45] test set in Tab. A.3.

Evaluation metrics In Sec. 4.1 we explained two compound metrics for the evaluation of MOT results, namely, Multi-Object Tracking Accuracy (MOTA) and Identity F1 score (IDF1). [5] However, the MOTChallenge benchmark implements all CLEAR MOT [5] evaluation metrics. In addition to MOTA and IDF1, we report the following additional CLEAR MOT metrics:

- MT: Ground truth tracks covered for at least 80%.
- ML: Ground truth tracks covered for at most 20%.
- FP: False positive bounding boxes not corresponding to any ground truth.
- FN: False negative ground truth boxes not covered by any bounding box.
- ID Sw.: Bounding box switching the corresponding ground truth identity. in the previous frame.
- sMOTSA: Mask-based Multi-Object Tracking Accuracy (MOTA) which counts true positives instead of only masks with IoU larger than 0.5.

Sequence	Public detection	MOTA \uparrow	IDF1 \uparrow	MT \uparrow	ML \downarrow	FP \downarrow	FN \downarrow	ID Sw. \downarrow
MOT17-01	DPM [14]	55.9	46.4	8	6	364	2439	39
MOT17-03	DPM	69.9	66.0	76	14	5774	25605	175
MOT17-06	DPM	60.4	61.5	87	52	880	3646	142
MOT17-07	DPM	60.4	49.2	16	10	965	5588	143
MOT17-08	DPM	42.3	41.4	19	21	720	11306	162
MOT17-12	DPM	54.4	61.1	38	28	802	3106	44
MOT17-14	DPM	39.9	46.8	27	44	1905	8954	256
MOT17-01	FRCNN [34]	52.0	43.9	8	7	474	2578	42
MOT17-03	FRCNN	71.1	67.5	78	14	5591	24464	181
MOT17-06	FRCNN	62.6	61.8	92	41	1026	3213	164
MOT17-07	FRCNN	59.0	49.6	16	6	1116	5661	153
MOT17-08	FRCNN	42.3	41.2	18	21	706	11341	149
MOT17-12	FRCNN	55.7	61.7	34	28	697	3100	45
MOT17-14	FRCNN	40.0	46.5	30	41	2186	8628	272
MOT17-01	SDP [48]	57.1	46.8	10	5	404	2324	41
MOT17-03	SDP	71.5	67.2	80	14	5670	24026	184
MOT17-06	SDP	61.5	61.2	95	49	1007	3370	156
MOT17-07	SDP	59.9	49.4	17	6	1086	5552	140
MOT17-08	SDP	44.0	42.5	19	20	724	10934	162
MOT17-12	SDP	54.9	61.4	35	26	839	3027	46
MOT17-14	SDP	40.6	47.3	31	43	2290	8408	286
All		61.8	59.8	834	496	35226	177270	2982

Table A.4. We report TrackFormer results on each individual sequence and set of public detections evaluated on the **MOT17** [27] test set. We apply the same **center distance** public detection filtering as in [53]. The arrows indicate low or high optimal metric values.

Sequence	Public detection	MOTA \uparrow	IDF1 \uparrow	MT \uparrow	ML \downarrow	FP \downarrow	FN \downarrow	ID Sw. \downarrow
MOT17-01	DPM [14]	51.5	46.6	8	8	278	2821	28
MOT17-03	DPM	67.3	64.4	67	16	5481	28584	172
MOT17-06	DPM	56.0	58.6	67	74	611	4452	117
MOT17-07	DPM	56.8	48.2	11	11	789	6377	137
MOT17-08	DPM	39.6	40.5	14	24	579	12039	133
MOT17-12	DPM	53.2	60.9	28	31	528	3493	34
MOT17-14	DPM	36.1	44.7	23	55	1505	10108	199
MOT17-01	FRCNN [34]	52.5	43.6	8	7	273	2754	40
MOT17-03	FRCNN	68.5	66.9	68	15	5279	27573	159
MOT17-06	FRCNN	61.5	61.8	77	49	770	3625	144
MOT17-07	FRCNN	55.4	48.6	12	9	869	6513	150
MOT17-08	FRCNN	39.5	40.2	14	24	569	12095	121
MOT17-12	FRCNN	48.7	58.0	17	39	477	3936	31
MOT17-14	FRCNN	36.8	43.8	22	45	1958	9516	212
MOT17-01	SDP [48]	57.0	48.6	8	5	353	2379	41
MOT17-03	SDP	71.2	67.3	76	15	5292	24728	179
MOT17-06	SDP	60.6	60.8	87	56	840	3654	144
MOT17-07	SDP	58.4	48.5	16	7	958	5921	141
MOT17-08	SDP	41.9	41.6	18	24	636	11491	148
MOT17-12	SDP	52.4	60.4	26	30	709	3387	33
MOT17-14	SDP	40.2	46.8	29	48	1970	8874	216
All		59.7	59.0	696	592	30724	194320	2579

Table A.5. We report TrackFormer results on each individual sequence and set of public detections evaluated on the **MOT17** [27] test set. We apply our **minimum intersection over union (IoU)** public detection filtering. The arrows indicate low or high optimal metric values.

References

- [1] Alexandre Alahi, Kratharth Goel, Vignesh Ramanathan, Alexandre Robicquet, Li Fei-Fei, and Silvio Savarese. Social lstm: Human trajectory prediction in crowded spaces. *IEEE Conf. Comput. Vis. Pattern Recog.*, 2016. [2](#)
- [2] Anton Andriyenko and Konrad Schindler. Multi-target tracking by continuous energy minimization. *IEEE Conf. Comput. Vis. Pattern Recog.*, 2011. [2](#)
- [3] Jerome Berclaz, Francois Fleuret, Engin Turetken, and Pascal Fua. Multiple object tracking using k-shortest paths optimization. *IEEE Trans. Pattern Anal. Mach. Intell.*, 2011. [2](#)
- [4] Philipp Bergmann, Tim Meinhardt, and Laura Leal-Taixé. Tracking without bells and whistles. In *Int. Conf. Comput. Vis.*, 2019. [1](#), [2](#), [7](#), [8](#), [11](#)
- [5] Keni Bernardin and Rainer Stiefelhagen. Evaluating multiple object tracking performance: the clear mot metrics. *EURASIP Journal on Image and Video Processing*, 2008, 2008. [6](#), [11](#)
- [6] Guillem Brasó and Laura Leal-Taixé. Learning a neural solver for multiple object tracking. In *IEEE Conf. Comput. Vis. Pattern Recog.*, 2020. [1](#), [2](#), [7](#), [8](#), [9](#), [11](#)
- [7] Nicolas Carion, F. Massa, Gabriel Synnaeve, Nicolas Usunier, Alexander Kirillov, and Sergey Zagoruyko. End-to-end object detection with transformers. *Eur. Conf. Comput. Vis.*, 2020. [1](#), [2](#), [3](#), [4](#), [6](#), [8](#), [9](#)
- [8] Long Chen, Haizhou Ai, Zijie Zhuang, and Chong Shang. Real-time multiple people tracking with deeply learned candidate selection and person re-identification. In *Int. Conf. Multimedia and Expo*, 2018. [1](#), [2](#), [7](#), [8](#), [11](#)
- [9] Wongun Choi and Silvio Savarese. Multiple target tracking in world coordinate with single, minimally calibrated camera. *Eur. Conf. Comput. Vis.*, 2010. [2](#)
- [10] Peng Chu and Haibin Ling. Famnet: Joint learning of feature, affinity and multi-dimensional assignment for online multiple object tracking. In *Int. Conf. Comput. Vis.*, 2019. [2](#), [7](#), [11](#)
- [11] Qi Chu, Wanli Ouyang, Hongsheng Li, Xiaogang Wang, Bin Liu, and Nenghai Yu. Online multi-object tracking using cnn-based single object tracker with spatial-temporal attention mechanism. In *Proceedings of the IEEE International Conference on Computer Vision*, pages 4836–4845, 2017. [2](#)
- [12] Patrick Dendorfer, Aljosa Osep, Anton Milan, Daniel Cremers, Ian Reid, Stefan Roth, and Laura Leal-Taixé. Motchallenge: A benchmark for single-camera multiple target tracking. *Int. J. Comput. Vis.*, 2020. [1](#)
- [13] Christoph Feichtenhofer, Axel Pinz, and Andrew Zisserman. Detect to track and track to detect. In *ICCV*, 2017. [2](#)
- [14] Pedro F. Felzenszwalb, Ross B. Girshick, David A. McAllester, and Deva Ramanan. Object detection with discriminatively trained part based models. *IEEE Trans. Pattern Anal. Mach. Intell.*, 2009. [6](#), [11](#), [12](#)
- [15] Kaiming He, Georgia Gkioxari, Piotr Dollár, and Ross Girshick. Mask r-cnn. In *IEEE Conf. Comput. Vis. Pattern Recog.*, 2017. [2](#), [7](#)
- [16] Kaiming He, Xiangyu Zhang, Shaoqing Ren, and Jian Sun. Deep residual learning for image recognition. In *IEEE Conf. Comput. Vis. Pattern Recog.*, 2016. [1](#), [3](#), [6](#), [9](#)
- [17] Roberto Henschel, Laura Leal-Taixé, Daniel Cremers, and Bodo Rosenhahn. Improvements to frank-wolfe optimization for multi-detector multi-object tracking. In *IEEE Conf. Comput. Vis. Pattern Recog.*, 2017. [1](#), [2](#), [7](#), [11](#)
- [18] Andrea Hornakova, Roberto Henschel, Bodo Rosenhahn, and Paul Swoboda. Lifted disjoint paths with application in multiple object tracking. In *Int. Conf. Mach. Learn.*, 2020. [2](#), [7](#), [11](#)
- [19] Hao Jiang, Sidney S. Fels, and James J. Little. A linear programming approach for multiple object tracking. *IEEE Conf. Comput. Vis. Pattern Recog.*, 2007. [2](#)
- [20] Margret Keuper, Siyu Tang, Bjoern Andres, Thomas Brox, and Bernt Schiele. Motion segmentation & multiple object tracking by correlation co-clustering. In *IEEE Trans. Pattern Anal. Mach. Intell.*, 2018. [1](#), [2](#), [7](#), [11](#)
- [21] Chanho Kim, Fuxin Li, Arridhana Ciptadi, and James M. Rehg. Multiple hypothesis tracking revisited. In *Int. Conf. Comput. Vis.*, 2015. [1](#), [2](#), [7](#), [11](#)
- [22] Laura Leal-Taixé, Cristian Canton-Ferrer, and Konrad Schindler. Learning by tracking: siamese cnn for robust target association. *IEEE Conf. Comput. Vis. Pattern Recog. Worksh.*, 2016. [1](#), [2](#)
- [23] Laura Leal-Taixé, Michele Fenzi, Alina Kuznetsova, Bodo Rosenhahn, and Silvio Savarese. Learning an image-based motion context for multiple people tracking. *IEEE Conf. Comput. Vis. Pattern Recog.*, 2014. [2](#)
- [24] Laura Leal-Taixé, Gerard Pons-Moll, and Bodo Rosenhahn. Everybody needs somebody: Modeling social and grouping behavior on a linear programming multiple people tracker. *Int. Conf. Comput. Vis. Workshops*, 2011. [1](#), [2](#)
- [25] Tsung-Yi Lin, Michael Maire, Serge Belongie, Lubomir Bourdev, Ross Girshick, James Hays, Pietro Perona, Deva Ramanan, C. Lawrence Zitnick, and Piotr Dollár. Microsoft coco: Common objects in context. *arXiv:1405.0312*, 2014. [6](#), [9](#)
- [26] Qiankun Liu, Qi Chu, Bin Liu, and Nenghai Yu. Gsm: Graph similarity model for multi-object tracking. In *Int. Joint Conf. Art. Int.*, 2020. [1](#), [2](#), [7](#), [11](#)
- [27] Anton Milan, Laura Leal-Taixé, Ian D. Reid, Stefan Roth, and Konrad Schindler. Mot16: A benchmark for multi-object tracking. *arXiv:1603.00831*, 2016. [2](#), [6](#), [7](#), [8](#), [9](#), [11](#), [12](#)
- [28] Anton Milan, Laura Leal-Taixé, Ian D. Reid, Stefan Roth, and Konrad Schindler. Mot16: A benchmark for multi-object tracking. *arXiv:1603.00831*, 2016. [5](#), [6](#)
- [29] Aljoša Ošep, Wolfgang Mehner, Paul Voigtlaender, and Bastian Leibe. Track, then decide: Category-agnostic vision-based multi-object tracking. *IEEE Int. Conf. Rob. Aut.*, 2018. [2](#)
- [30] Niki Parmar, Ashish Vaswani, Jakob Uszkoreit, Łukasz Kaiser, Noam Shazeer, Alexander Ku, and Dustin Tran. Image transformer. *arXiv preprint arXiv:1802.05751*, 2018. [2](#)
- [31] Stefano Pellegrini, Andreas Ess, Konrad Schindler, and Luc Van Gool. You'll never walk alone: modeling social behavior for multi-target tracking. *Int. Conf. Comput. Vis.*, 2009. [2](#)

- [32] Hamed Pirsiavash, Deva Ramanan, and Charless C. Fowlkes. Globally-optimal greedy algorithms for tracking a variable number of objects. *IEEE Conf. Comput. Vis. Pattern Recog.*, 2011. [2](#)
- [33] Lorenzo Porzi, Markus Hofinger, Idoia Ruiz, Joan Serrat, Samuel Rota Buló, and Peter Kotschieder. Learning multi-object tracking and segmentation from automatic annotations. In *IEEE Conf. Comput. Vis. Pattern Recog.*, 2020. [2](#), [7](#)
- [34] Shaoqing Ren, Kaiming He, Ross Girshick, and Jian Sun. Faster r-cnn: Towards real-time object detection with region proposal networks. *Adv. Neural Inform. Process. Syst.*, 2015. [1](#), [6](#), [12](#)
- [35] Hamid Rezaatoughi, Nathan Tsoi, JunYoung Gwak, Amir Sadeghian, Ian Reid, and Silvio Savarese. Generalized intersection over union: A metric and a loss for bounding box regression. In *IEEE Conf. Comput. Vis. Pattern Recog.*, 2019. [3](#)
- [36] Ergys Ristani, Francesco Solera, Roger S. Zou, Rita Cucchiara, and Carlo Tomasi. Performance measures and a data set for multi-target, multi-camera tracking. In *Eur. Conf. Comput. Vis. Workshops*, 2016. [6](#)
- [37] Ergys Ristani and Carlo Tomasi. Features for multi-target multi-camera tracking and re-identification. *IEEE Conf. Comput. Vis. Pattern Recog.*, 2018. [2](#)
- [38] Alexandre Robicquet, Amir Sadeghian, Alexandre Alahi, and Silvio Savarese. Learning social etiquette: Human trajectory prediction. *Eur. Conf. Comput. Vis.*, 2016. [2](#)
- [39] Paul Scovanner and Marshall F. Tappen. Learning pedestrian dynamics from the real world. *Int. Conf. Comput. Vis.*, 2009. [2](#)
- [40] Shuai Shao, Zijian Zhao, Boxun Li, Tete Xiao, Gang Yu, Xiangyu Zhang, and Jian Sun. Crowdhuman: A benchmark for detecting human in a crowd. *arXiv:1805.00123*, 2018. [6](#), [8](#)
- [41] H. Sheng, Y. Zhang, J. Chen, Z. Xiong, and J. Zhang. Heterogeneous association graph fusion for target association in multiple object tracking. *IEEE Transactions on Circuits and Systems for Video Technology*, 2019. [2](#), [7](#), [11](#)
- [42] Russell Stewart, Mykhaylo Andriluka, and Andrew Y Ng. End-to-end people detection in crowded scenes. In *Proceedings of the IEEE conference on computer vision and pattern recognition*, pages 2325–2333, 2016. [2](#), [3](#)
- [43] Siyu Tang, Mykhaylo Andriluka, Bjoern Andres, and Bernt Schiele. Multiple people tracking by lifted multicut and person re-identification. In *IEEE Conf. Comput. Vis. Pattern Recog.*, 2017. [2](#)
- [44] Ashish Vaswani, Noam Shazeer, Niki Parmar, Jakob Uszkoreit, Llion Jones, Aidan N Gomez, Łukasz Kaiser, and Illia Polosukhin. Attention is all you need. In *Adv. Neural Inform. Process. Syst.*, 2017. [1](#), [2](#), [3](#), [4](#), [6](#)
- [45] Paul Voigtlaender, Michael Krause, Aljosa Osep, Jonathon Luiten, Berin Balachandar Gnana Sekar, Andreas Geiger, and Bastian Leibe. Mots: Multi-object tracking and segmentation. In *IEEE Conf. Comput. Vis. Pattern Recog.*, 2019. [2](#), [5](#), [6](#), [7](#), [8](#), [9](#), [11](#)
- [46] Zhenbo Xu, Wei Zhang, Xiao Tan, Wei Yang, Huan Huang, Shilei Wen, Errui Ding, and Liusheng Huang. Segment as points for efficient online multi-object tracking and segmentation. In *Eur. Conf. Comput. Vis.*, 2020. [2](#), [7](#)
- [47] Kota Yamaguchi, Alexander C. Berg, Luis E. Ortiz, and Tamara L. Berg. Who are you with and where are you going? *IEEE Conf. Comput. Vis. Pattern Recog.*, 2011. [2](#)
- [48] Fan Yang, Wongun Choi, and Yuanqing Lin. Exploit all the layers: Fast and accurate cnn object detector with scale dependent pooling and cascaded rejection classifiers. *IEEE Conf. Comput. Vis. Pattern Recog.*, 2016. [6](#), [11](#), [12](#)
- [49] Fan Yang, Wongun Choi, and Yuanqing Lin. Exploit all the layers: Fast and accurate cnn object detector with scale dependent pooling and cascaded rejection classifiers. *IEEE Conf. Comput. Vis. Pattern Recog.*, pages 2129–2137, 2016. [7](#)
- [50] Qian Yu, Gerard Medioni, and Isaac Cohen. Multiple target tracking using spatio-temporal markov chain monte carlo data association. *IEEE Conf. Comput. Vis. Pattern Recog.*, 2007. [2](#)
- [51] Li Zhang, Yuan Li, and Ramakant Nevatia. Global data association for multi-object tracking using network flows. *IEEE Conference on Computer Vision and Pattern Recognition (CVPR)*, 2008. [2](#)
- [52] Y. Zhang, H. Sheng, Y. Wu, S. Wang, W. Lyu, W. Ke, and Z. Xiong. Long-term tracking with deep tracklet association. *IEEE Trans. Image Process.*, 2020. [2](#), [7](#), [11](#)
- [53] Xingyi Zhou, Vladlen Koltun, and Philipp Krähenbühl. Tracking objects as points. *ECCV*, 2020. [2](#), [5](#), [6](#), [7](#), [8](#), [10](#), [11](#), [12](#)
- [54] Ji Zhu, Hua Yang, Nian Liu, Minyoung Kim, Wenjun Zhang, and Ming-Hsuan Yang. Online multi-object tracking with dual matching attention networks. In *Eur. Conf. Comput. Vis.*, 2018. [2](#)